THE JOURNAL OF PHYSICAL CHEMISTRY A

ARTICLE

pubs.acs.org/JPCA

Measuring Molecular Dynamics and Activation Energies for Quaternary Acyclic Ammonium and Cyclic Pyrrolidinium Ionic Liquids Using ^{14}N NMR Spectroscopy

Todd M. Alam,[†] Daniel R. Dreyer,[‡] Christopher W. Bielwaski,[‡] and Rodney S. Ruoff[§]

[†]Department of Electronic and Nanostructured Materials, Sandia National Laboratories, Albuquerque, New Mexico 87185-0886, United States

[‡]Department of Chemistry and Biochemistry, The University of Texas at Austin, One University Station, A5300, Austin, Texas 78712, United States

[§]Department of Mechanical Engineering and the Texas Materials Institute, The University of Texas at Austin, One University Station, C2200, Austin, Texas 78712, United States

Supporting Information

ABSTRACT: The ^{14}N NMR spin−lattice (R_1) and spin−spin (R_2) relaxation rates were determined as a function of temperature for a series of tetra-alkyl acyclic ammonium and cyclic pyrrolidinium ionic liquids (ILs). Through the use of the R_2/R_1 ratio method, it was shown that for the majority of these ILs, the reorientational dynamics are not in the extreme narrowing regime, but instead are in the dispersive relaxation regime, thus allowing a unique solution for the correlation time to be determined. The temperature variation of the R_2 relaxation rate, along with the temperature variation of the calculated correlation times, allowed activation energies for the reorientational dynamics to be measured and compared. In addition, these NMR relaxation experiments enabled the ^{14}N quadrupolar coupling product to be extracted, which revealed surprising temperature dependence. Collectively, the ^{14}N NMR results allow the impact of cation and anion identity on the local reorientational dynamics of these ILs to be delineated.

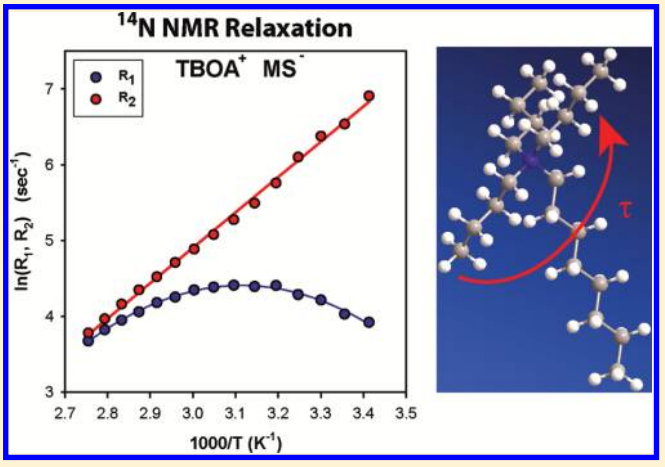

INTRODUCTION

Ionic liquids (ILs) continue to see extensive interest for a wide range of material science applications ranging from liquid electrolytes for energy storage and production,[1−3] CO_2 capture,[4] green chemistry,[5,6] lubricant fluids,[7] biomass processing,[8] nanostructured synthesis,[9,10] and catalysis.[11] A deeper understanding of the structure and dynamics, and the related physicochemical properties in ILs is still required to optimize for future applications. Even though there have been numerous structural studies using a variety of different techniques,[12−16] questions still remain about the supramolecular organization of ionic liquids, including the role of dynamics, ion pairing, hydrogen bonding, and the interaction of ILs with solutes or solvents. Variations in the IL structure and dynamics due to surface interactions during thin film formation or confinement in nanoporous materials have also been noted, but still require additional characterization.

NMR spectroscopy is a powerful tool to probe the dynamics and structure in ILs.[17] Numerous studies have been reported, including the use of solution ^{1}H, ^{2}H, ^{13}C, ^{15}N, and ^{19}F NMR.[18−22] Pulse-field-gradient (PFG) NMR spectroscopy has also been used to measure the self-diffusion rates of ILs, providing insight into the factors controlling electrochemical conductivity,[23−27] the role water has on IL diffusion,[28] and the decrease in IL diffusivity within nanoporous membranes.[29] Solid state NMR spectroscopy has been utilized to probe the interactions of ILs with material surfaces, including confinement in mesoporous silica,[30] silica ionogels,[31] or film formation on metal and ceramic surfaces.[32]

Investigations involving ^{14}N NMR spectroscopy to characterize ILs have been more limited, which is somewhat surprising given the fact that the natural abundance of ^{14}N is high (99.63%), and both cations and anions in several classes of ILs contain significant amounts of nitrogen. These limited studies include the ^{14}N NMR spectroscopy of neat diethylpyridinium bromide, $[DEP]^+Br^-$,[33] along with a study of ILs immobilized on silica,

Received: January 20, 2011
Revised: March 10, 2011
Published: April 01, 2011

where the line width was used to obtain qualitative information about local ionic mobility and the role solvent has on disrupting the IL's structure.[34] The paucity of ^{14}N NMR studies is primarily due to nitrogen being a quadrupolar nucleus ($I = 1$), where the large quadrupolar coupling constant (QCC) can produce significant line broadening and loss of signal.

In this work, we present ^{14}N NMR data for a series of ILs containing quaternary ammonium or pyrrolidinium cations, where the symmetry around the nitrogen results in a nominal QCC, such that the corresponding NMR spectra exhibited relatively narrow line widths and were easily obtained. These classes of ILs are of interest because they exhibit electrochemical stability over a wide potential range,[35,36] and are being investigated for energy storage capabilities. By analyzing both spin−lattice (R_1) and spin−spin (R_2) relaxation rates, the molecular reorientation correlation times (τ) were directly determined, and followed as a function of temperature. The Arrhenius behaviors of these molecular correlation times were also evaluated.

EXPERIMENTAL SECTION

^{14}N NMR Relaxation Experiments. To reduce the impact of residual water, all ionic liquids were sealed in 5 mm NMR tubes prior to storage and analysis (see additional preparation details below). All ^{14}N NMR experiments were performed on a Bruker Avance-III 600 spectrometer at 43.35 MHz using a 5 mm broadband probe. The longitudinal spin−lattice ($R_1 = 1/T_1$) and transverse spin−spin ($R_2 = 1/T_2$) relaxation rates (which are the inverse of the relaxation times T_1 and T_2, respectively) were obtained using an inversion recovery and a CPMG (Carr−Purcell−Meiboom−Gill) pulse sequence with 32 recovery delays, 8 scans, and a 500 ms recycle time. Variable temperature experiments were obtained with ±0.1 °C accuracy, following a temperature calibration using the 1,2-ethanediol method.[37] The ^{14}N NMR chemical shifts (δ) were referenced to the secondary external reference nitromethane, δ = +381 ppm with respect to liquid ammonia (δ = 0 ppm) at 25 °C. A single exponential decay was observed for both R_1 and R_2 for all samples over the entire temperature range investigated. The extraction of the reorientational correlation times from the relaxation rates is described below.

Preparation of Ionic Liquids, General Considerations. The structures of the various ILs explored are shown in Figure 1. The ILs *N,N,N*-tri(*n*-butyl)-*N*-(*n*-octyl) ammonium bis(trifluoromethanesulfonyl)imide ($[TBOA]^+TFSI^-$),[1,38,39] and *N*-methyl-*N*-(*n*-octyl)pyrrolidinium bis(trifluoromethanesulfonyl) imide ($[MOPyrr]^+TFSI^-$),[1] were synthesized according to previously reported procedures. The synthetic details are included in the Supporting Information for comparison. The IL *N*-methyl-*N*-(*n*-butyl)pyrrolidinium bis(trifluoromethanesulfonyl) imide ($[MBPyrr]^+TFSI^-$) was obtained directly from Sigma Aldrich and was used without further preparation. All other reagents were purchased from Acros Organics, TCI America, or Alfa Aesar, and were distilled prior to use. Unless otherwise noted, all reactions were performed under ambient conditions. Prior to NMR analysis, all ILs were dried under vacuum (10^{-3} Torr) at 100 °C for 24 h. The samples were then transferred under static vacuum to an inert N_2 atmosphere drybox and loaded into 5 mm NMR tubes, which were then removed from the drybox and immediately flame-sealed. Solution ^{1}H and ^{13}C NMR spectroscopy was used to check the identity and purity; spectroscopic data were collected on Varian Unity INOVA 400 MHz and Varian Mercury 300 MHz

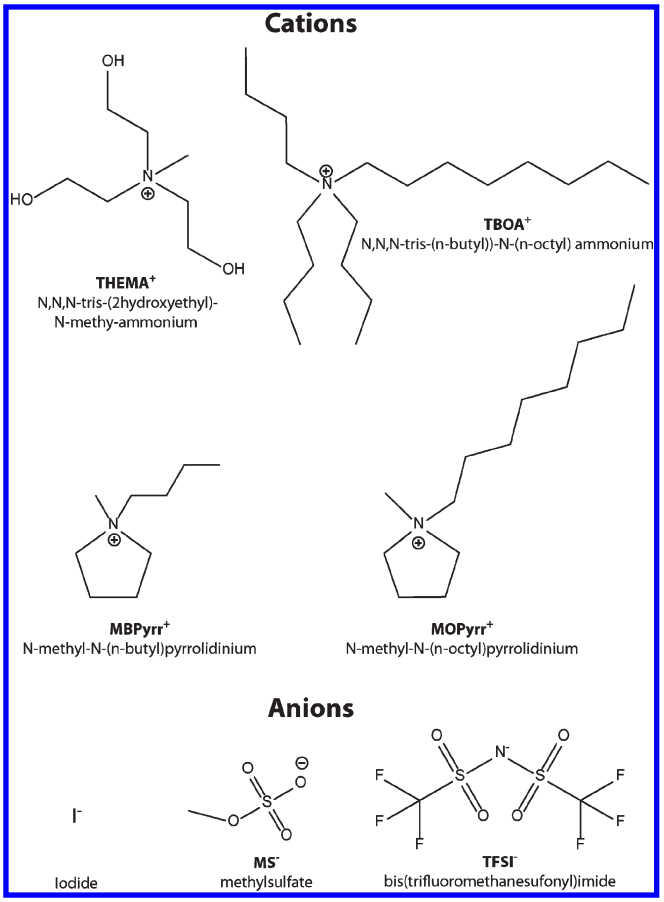

Figure 1. The quaternary acyclic ammonium and cyclic pyrrolidinium cations along with the selected anions used for the ionic liquids investigated here.

spectrometers. Chemical shifts (δ) were referenced downfield from $(CH_3)_4Si$ using the residual solvent peak as an internal standard ($CDCl_3$, +7.24 ppm for ^{1}H and +77.0 ppm for ^{13}C NMR, respectively; DMSO-d_6, +2.49 ppm for ^{1}H and +39.5 ppm for ^{13}C NMR, respectively). High-resolution mass spectra (HRMS) were obtained with a VG analytical ZAB2-E instrument (ESI or CI). Unless otherwise noted, all glass transition temperatures (T_g) and/or melting points (T_m) were measured using a Mettler Toledo DSC 823e. Decomposition temperatures (T_d) were obtained using a Mettler Toledo TGA/SDTA 851. Elemental analyses were performed by Midwest Microlabs, LLC (Indianapolis, IN).

***N,N,N*-Tri(*n*-butyl)-*N*-(*n*-octyl)ammonium Methylsulfate, $[TBOA]^+MS^-$.** A 40-mL vial was charged with *N,N,N*-tributyl-*N*-octylammonium bromide (3.43 g, 9.05×10^{-3} mol), acetonitrile (30 mL) and a magnetic stir bar. The resulting mixture was cooled to 0 °C on an ice bath. Dimethyl sulfate (1.21 g, 9.56×10^{-3} mol) was added slowly to the open vial and the mixture was stirred for 1 h at 0 °C, after which time the mixture was slowly brought to room temperature and stirred for an additional 6 h. The solvent was then removed under vacuum and the resulting pale yellow liquid was washed with diethyl ether (3×30 mL). Residual solvent was removed under high vacuum which afforded the desired product as a yellow liquid (3.63 g, 98%). ^{1}H NMR (400 MHz, $CDCl_3$): 3.64 (s, 3H), 3.22 (t, 8H), 2.60 (m, 8H), 1.21−1.44 (m, 16H), 0.94 (t, 9H), 0.82 (t, 3H). ^{13}C NMR (75 MHz, $CDCl_3$): 58.5, 54.2, 31.5, 29.0, 28.91, 26.21,

23.81, 22.5, 21.9, 19.6, 14.0, 13.6. T_g = −49.3 °C. T_d = 266.3 °C. HRMS Calcd. for $C_{20}H_{44}N$ [M^+]: 298.3475. Found: 298.3474. Anal. Calcd. for $C_{21}H_{47}NO_4S$: C, 61.57; H, 11.56; N, 3.42. Found: C, 61.55; H, 11.48; N, 3.51.

***N*-Methyl-*N*-(*n*-octyl)pyrrolidinium Methylsulfate, [MOPyrr]$^+$MS$^-$.** A 40-mL vial was charged with *N*-methyl-*N*-octylpyrrolidinium bromide (3.94 g, 1.42 × 10^{-2} mol), acetonitrile (40 mL), and a magnetic stir bar. The solution was then cooled to 0 °C on an ice bath. Dimethyl sulfate (2.17 g, 1.72 × 10^{-2} mol) was slowly added while stirring. The mixture was stirred at 0 °C for 1 h, after which time it was slowly brought to room temperature and stirred for an additional 6 h. The solvent was then removed under vacuum and the resulting pale yellow liquid was washed with diethyl ether (3 × 30 mL). Residual solvent was removed under high vacuum which afforded the desired product as a pale yellow liquid (4.35 g, 99%). ^{1}H NMR (400 MHz, $CDCl_3$): 3.58 (s, 3H), 3.54 (t, 4H), 3.33 (t, 2H), 3.04 (s, 3H), 2.16 (br, 4H), 1.65 (br, 2H), 1.24 (br, 4H), 1.17 (m, 6H), 0.77 (t, 3H). ^{13}C NMR (75 MHz, $CDCl_3$): 64.0, 54.0, 48.0, 31.4, 28.9, 28.8, 26.2, 23.7, 22.3, 21.4, 13.8. T_g = −71.8 °C. T_d = 265.3 °C. HRMS Calcd. for $C_{13}H_{28}N$ [M^+]: 198.2222. Found: 198.2222. Anal. Calcd. for $C_{14}H_{31}NO_4S$: C, 54.34; H, 10.10; N, 4.53. Found: C, 54.41; H, 10.27; N, 4.70.

***N,N,N*-Tris-(2-hydroxyethyl)-*N*-methylammonium Iodide, [THEMA]$^+$I$^-$.** A 40-mL vial was charged with triethanolamine (3.17 g, 2.12 × 10^{-2} mol), CH_2Cl_2 (30 mL), and a magnetic stir bar. Methyl iodide (3.14 g, 2.22 × 10^{-2} mol) was added to this solution and the vial was sealed with a Teflon-lined cap. The mixture was stirred at room temperature for 1 h, and then brought to 40 °C for 10 h. During this time, a clear colorless phase separation was observed. The supernatant was decanted away and the mixture was washed with CH_2Cl_2 (3 × 20 mL). Residual solvent was removed under high vacuum which afforded the desired product as a colorless liquid (6.05 g, 98%). ^{1}H NMR (400 MHz, DMSO-d_6): 5.161 (t, 3H), 3.82 (m, 6H), 3.51 (t, 6H), 3.12 (s, 3H). ^{13}C NMR (75 MHz, DMSO-d_6): 64.1, 54.9, 49.7. T_g = −73.3 °C. T_d = 227.4 °C. HRMS Calcd. for $C_7H_{18}NO_3$ [M^+]: 164.1289. Found: 164.1287. Anal. Calcd. for $C_7H_{18}INO_3$: C, 28.88; H, 6.23; N, 4.81. Found: C, 28.71; H, 6.36; N, 4.73.

***N,N,N*-Tris-(2-hydroxyethyl)-*N*-methylammonium Methylsulfate, [THEMA]$^+$MS$^-$.** A 40-mL vial was charged with triethanolamine (4.24 g, 2.84 × 10^{-2} mol), acetonitrile (30 mL), and a magnetic stir bar, and the mixture was cooled to 0 °C in an ice bath. Dimethyl sulfate (3.73 g, 2.96 × 10^{-2} mol) was slowly added to the resulting mixture while stirring. The mixture was stirred at 0 °C for 1 h, after which time it was slowly brought to room temperature and stirred for an additional 12 h. A clear, pale yellow phase separation was observed and the supernatant was decanted away. The resulting pale yellow liquid was washed with acetonitrile (3 × 30 mL). Residual solvent was removed under high vacuum which afforded the desired product as a viscous, pale yellow liquid (7.74 g, 99%). ^{1}H NMR (400 MHz, DMSO-d_6): 4.84 (br, 3 H), 3.82 (m, 6H), 3.51 (t, 6H), 3.37 (s, 3H), 3.12 (s, 3H). ^{13}C NMR (75 MHz, DMSO-d_6): 64.3, 55.0, 53.1, 49.8. T_g = −46.5 °C. T_d = 303.6 °C. HRMS Calcd. for $C_7H_{18}NO_3$ [M^+]: 164.1290. Found: 164.1287. Anal. Calcd. for $C_8H_{21}NO_7S$: C, 34.90; H, 7.69; N, 5.09. Found: C, 34.76; H, 7.58; N, 5.14.

Theoretical Background. The ^{14}N NMR R_1 and R_2 NMR relaxation rates are dominated by the quadrupolar relaxation mechanism and involve the coupling between the quadrupolar moment of the nitrogen nucleus (eQ) and electrical field gradient (EFG) tensor. Fluctuations of the EFG give rise to the observed NMR relaxation, with the relaxation rates defined by the following:[40]

$$\begin{aligned} R_1 &= K[2J(\omega_0) + 8J(2\omega_0)] \\ R_2 &= K[3J(0) + 5J(\omega_0) + 2J(2\omega_0)] \end{aligned} \quad (1)$$

where $J(n\omega_0)$ are spectral densities that are a function of the experimental Larmor frequency ($\omega_0 = 2\pi \cdot 43.35$ MHz). The interaction parameters are given by

$$K = \frac{3\pi^2 P_Q^2}{40}, P_Q = \frac{e^2 qQ}{h}\sqrt{1 + \frac{\eta_Q^2}{3}} \quad (2)$$

with the quadrupolar product (P_Q) combines terms involving QCC (=$(e^2qQ)/(h)$) and the EFG asymmetry parameter ($0 \leq \eta_Q \leq 1$). The NMR relaxation experiments do not allow unique determination of η_Q or the sign of QCC, but the asymmetry produces, at most, a 15% variation in the coupling strength. The product P_Q will be reported throughout the remainder of the paper. Evaluation of $J(n\omega_0)$ typically requires the introduction of specific molecular models. Note eqs 1 and 2 are valid for any reorientational model as long as the system is in an isotropic equilibrium state. For isotropic molecular reorientation the spectral densities are given by the following:

$$J(\omega_0) = \frac{2\tau}{1 + (\omega_0\tau)^2} \quad (3)$$

where the correlation time τ defines the time constant for EFG tensor fluctuations. For small rigid molecules, τ commonly reflects the molecular reorientational time constant. For the ILs described here, τ is more accurately a combination of the molecular reorientation and motions of the nitrogen substituents (N−C bond rotations) that may produce changes in the EFG. More complex models can be introduced, including anisotropic molecular reorientation. The addition of anisotropic molecular diffusion results in additional fitting parameters including the three principal components of the diffusion tensor, along with the relative orientation of the EFG tensor with respect to diffusion tensor.[41,42] These more complicated motional models were not pursued in this work.

In the extreme narrowing limit ($\omega_0\tau \ll 1$) there are rapid molecular reorientations (for example in a nonviscous solution) with the spectral densities reducing to the following:

$$\begin{aligned} J(0) &= J(\omega_0) = J(2\omega_0) = 2\tau \\ R_1 &= R_2 \end{aligned} \quad (4)$$

Outside the extreme narrowing limit ($R_1 \neq R_2$) the determination of the correlation times and P_Q from a single relaxation measurement become intertwined. It has been shown that for systems with slower molecular reorientation a unique solution for τ can be realized from analysis of the R_2/R_1 ratio.[43,44] By combining eqs 1 and 3 a quadratic relation can be developed,[45,46]

$$X^2 + \left[\frac{37}{12} - \frac{2}{3}\left(\frac{2R_2}{R_1}\right)\right]X + \left[\frac{5}{6} - \frac{5}{12}\left(\frac{2R_2}{R_1}\right)\right] = 0 \quad (5)$$

where $X = \omega_0^2\tau^2$. A single positive root (for $R_2 > R_1$) for eq 5 is obtained, thus allowing the correlation time to be determined. Once τ has been measured, eq 1 was used to calculate P_Q.

Table 1. Activation Energies, Correlation Times and Quadrupolar Coupling Constant for Quaternary Acyclic Ammonia and Cyclic Pyrrolidinium Ionic Liquids Obtained from Analysis of the ^{14}N NMR Relaxation Data

sample	δ (fwhm)[a]	E_a (kJ mol^{-1})[b](r^2)	E_a (kJ mol^{-1})[c](r^2)	τ (ns)[d]	P_Q (kHz)[d]
THEMA$^+$ I$^-$	+60 (42)	40.0 ± 0.4(0.9994)	36 ± 3[e](0.9987)	2.2	71.4
THEMA$^+$ MS$^-$	+60 (130)	36.3 ± 0.4(0.9986)	32 ± 1[e](0.9961)	5.0	94.2
TBOA$^+$ MS$^-$	+67 (260)	38.8 ± 0.4(0.9971)	38.2 ± 0.4(0.9976)	13.6	100.8
TBOA$^+$ TFSI$^-$	+66 (35)	34.6 ± 0.3(0.9991)	39 ± 2[e](0.9988)	3.1	59.0
MBPyrr$^+$ TFSI$^-$	+74 (27)	29.2 ± 0.3(0.9956)	–[f]	–[f]	–[f]
MOPyrr$^+$ MS$^-$	+73 (115)	37.8 ± 0.4(0.9980)	32 ± 1[e](0.9924)	5.5	95.9
MOPyrr$^+$ TFSI$^-$	+73 (47)	28.9 ± 0.3(0.9992)	29.0 ± 0.3(0.9955)	2.5	73.1

[a] For neat IL samples at 25 °C. δ = chemical shift (ppm). fwhm = full width at half-maximum (Hz). [b] Energy of activation determined from R_2 (CPMG) temperature dependence, with the coefficient of determination r^2 given in parentheses. [c] Energy of activation determined from temperature dependence of extracted correlation times, with the coefficient of determination r^2 given in parentheses. [d] At 298 K. [e] Increased error due to limit range of correlation times. [f] Not in $R_2 > R_1$ relaxation rate regime.

RESULTS AND DISCUSSION

The ^{14}N NMR spectra of the various ILs examined (structures shown in Figure 1) revealed a single quadrupolar broadened resonance (spectra not shown) over the entire temperature range investigated (293 to 363 K). This range is significantly above the T_g for all ILs investigated, assuring that the observed reorientational dynamics are not impacted by this phase transition. Only a single nitrogen species is predicted for the alkyl ammonia and pyrrolidinium cations. The ^{14}N NMR chemical shifts (δ) and observed full width at half-maximum (fwhm) line widths are given in Table 1. The observed ^{14}N δ for the alkyl ammonia ILs ranged between +60 and +67 ppm, while the ^{14}N δ for the pyrrolidinium ILs were between +73 and +74 ppm. These chemical shift ranges were consistent with aliphatic type ammonium cations. As predicted, the identity of the anion in the IL had minimal impact on the observed ^{14}N NMR chemical shift of the cation. It should be noted that the ^{14}N NMR signal for the nitrogen in the TFSI$^-$ anion was also observed at the higher temperatures, but was significantly broadened. The ^{14}N NMR signal from this anion nitrogen was not analyzed, and did not interfere with the NMR relaxation experiments for the nitrogen-containing cations. While the ^{14}N δ can provide some information about the local bonding environment, the increased line width tends to mask subtle details (such as presence of hydrogen bonding) that otherwise might be observable using ^{15}N NMR spectroscopy.

The cation ^{14}N NMR line widths and R_2 relaxation rates were strongly dependent on the identity of the anion and therefore subject to changes in the cation reorientational dynamics (see discussion below). Variation of the ^{14}N NMR line width with temperature has also be used to extract a molecular reorientation energy of activation (E_a),[33] but analysis of line widths (and the corresponding R_2 relaxation rates) does not allow τ to be determined without previous knowledge of the quadrupolar coupling product (P_Q). We have therefore elected to utilize the combined analysis of the spin−spin R_2 relaxation rates (as determined from the CPMG pulse sequence) and the spin−lattice R_1 relaxation rates to directly evaluate the correlation times independent of P_Q as described in the Experimental Section.

Figure 2 shows the R_1 and R_2 relaxation rates for the acyclic ammonium ILs (THEMA$^+$I$^-$, THEMA$^+$MS$^-$, TBOA$^+$TFSI$^-$, and TBOA$^+$MS$^-$) as a function of temperature. At very high temperatures, $R_1 \approx R_2$, as would be predicted for the extreme narrowing limit ($\omega_0\tau \ll 1$). More interesting is that reorientations of these ILs are not in the extreme narrowing limit at room temperature, but instead are entering the dispersive relaxation regime with respect to the Larmor frequency (43 MHz). Occasionally, this is referred to as the "high viscosity regime"; this may be misleading since the reduced reorientational dynamics may result from not only from increases in the microviscosity, but from increased or new intermolecular interactions. While many previous studies have argued that the dynamics of other room temperature (RT) ILs were in the extreme narrowing limit, this assumption is clearly inappropriate for the examples presented here. As noted in the Experimental Section, the ^{14}N NMR quadrupolar relaxation mechanism is dominant for the ILs described above, allowing a detailed analysis of the aforementioned NMR data. The linear dependence of the R_2 relaxation rate with inverse temperature shows that this relaxation is still dominated by the zero frequency $J(0)$ spectral density (eq 1), and is directly proportional to the reorientational (or EFG fluctuation) correlation time. We have evaluated the Arrhenius activation energy (E_a) from the linear dependence of the R_2 relaxation (Table 1), even though this assumes the quadrupolar coupling product, P_Q, in eqs 1 and 2 is temperature independent. As discussed further below, this assumption does not hold for the present series of ILs, and that the E_a values obtained from evaluation of just the R_2 temperature variation are biased. The R_1 relaxation rate does not include the $J(0)$ spectral density, resulting in the distinct deviation from R_2 with decreasing temperatures, thus precluding the evaluation of E_a directly from the R_1 relaxation rates.

Similarly, the temperature variation of the R_1 and R_2 relaxation rates for the pyrrolidinium ILs is shown in Figure 3. The [MBPyrr]$^+$TFSI relaxation behavior is similar to previous ^{14}N NMR studies of diethylpyridinium bromide, [DEP]$^+$Br$^-$,[33] with $R_1 \approx R_2$ (extreme narrowing limit) over a similar temperature range, where the remainder of the pyrrolidinium ILs are in the dispersive relaxation regime. The E_a values obtained from the R_2 relaxation rates for the pyrrolidinium ILs are also provided in Table 1. The E_a range from 28.9 to 40.0 kJ/mol, and do not reveal any trends between being the acyclic ammonium-based and the cyclic pyrrolidinium-based cation. A decrease in E_a is observed with increasing the size of the anion from I$^-$ to TFSI$^-$. The activation energies for the acyclic ammonium and pyrrolidinium ILs are 3 to 4 times larger than the 10 kJ mol^{-1} previously reported for the [DEP]$^+$Br$^-$ IL.[33]

Direct Determination of Correlation Times. Using the R_2/R_1 relaxation rate ratio method, and eqs 1 and 5, a unique positive τ can be calculated from the observed ^{14}N NMR relaxation data. No assumptions were required in estimating the value of P_Q, as this

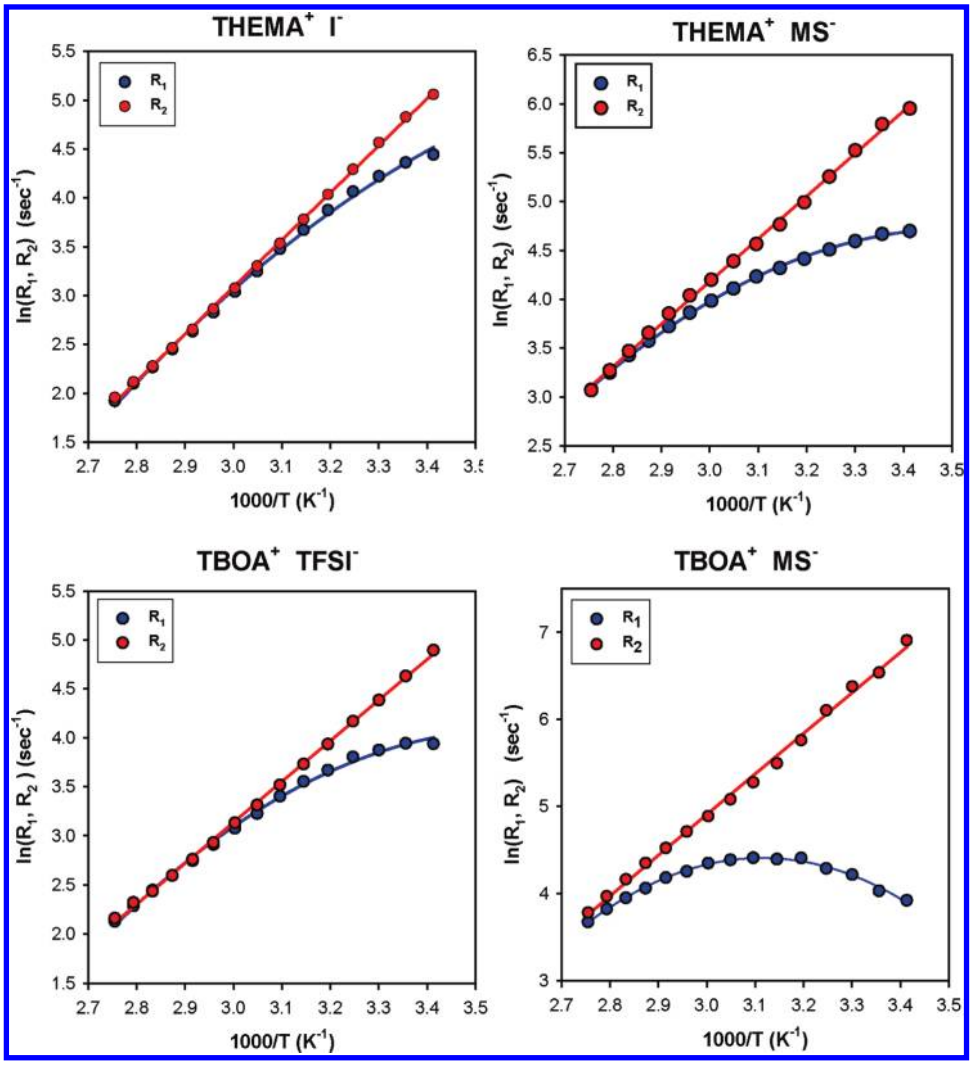

Figure 2. The ^{14}N NMR R_1 (= $1/T_1$) and R_2 (= $1/T_2$) relaxation rates as a function of temperature for different tetra-alkyl acyclic ammonium-based ILs. The linear regression to the R_2 relaxation rates allowed the reorientational activation energy (E_a) to be evaluated, while the nonlinear fit for R_1 is provided for visual aid only.

term is not present in the R_2/R_1 ratio. Figure 4 shows the temperature variation of these correlation times for the acyclic ILs. As the relaxation rate ratio approaches the extreme narrowing limit ($R_2 \approx R_1$), the error in τ increases significantly as the roots of eq 5 becomes poorly defined.[47] We have arbitrarily chosen a cutoff condition in which R_2 must be at least 5% larger than R_1 to allow a reliable determination of τ. Experimental points that fulfill the 5% cutoff are shown as solid circles in Figure 4, while those below this cutoff ($R_2 \approx R_1$) are shown as filled triangles. As a comparison, the determined correlation times at 25 °C for the different ILs are given in Table 1, and range from ~2 to 14 ns. Similarly, Figure 5 shows the temperature variation of τ for the pyrrolidinium based IL, with the 25 °C correlation times given in Table 1. For $[MBPyrr]^+TFSI^-$, the ^{14}N NMR relaxation was in the extreme narrowing limit over the entire temperature range and precluded the determination of τ for this compound. The slower reorientation of the $[MOPyrr]^+$ cations, compared to the $[MBPyrr]^+$ cation, resulted from the longer N-alkyl substituent or from changes in the cation−anion interactions.

These experimentally determined correlation times (ns) are significantly longer than the shorter ps correlation times commonly observed for liquids, consistent with the picture of slower reorientational dynamics in ILs. These longer correlation times reflect both the larger molecular size of the studied cations, and the presence of strong cation−anion (ion pair) interactions within ILs.[48] These measured results (Table 1) are of the same order of magnitude as the correlation times reported for a series of imidazoium ILs using ^{1}H and ^{13}C NMR relaxation (~3 ns),[22] ^{1}H and ^{19}F NMR (~1 ns),[49] and ^{2}H NMR (~ 40 ps).[19] Molecular dynamics (MD) simulations for liquid *N*-methyl-*N*-propylpyrrolidinium ($MPPyrr^+$) $TFSI^-$ have predicted a rotational relaxation time on the order of 0.3 ns, while MD simulations of the smaller *N*-*N*-diethyl-*N*-methylammonium triflate ionic liquid predicted rotational diffusion on the time scale of 2.5 ns: again on the same order of magnitude observed experimentally.

The validity of using an isotropic molecular reorientation model (eq 3) to extract a single correlation times also needs to be discussed. On one hand, molecular dynamics (MD) simulations for the ionic liquid *N*-ethyl-*N*,*N*,dimethyl-*N*-(2-methoxyethyl) ammonium ($NOENM_2E$) $TFSI^-$ predicts that both the cation and anion do not have significant anisotropic dynamics.[50] We argue that in the present work, the $THEMA^+$

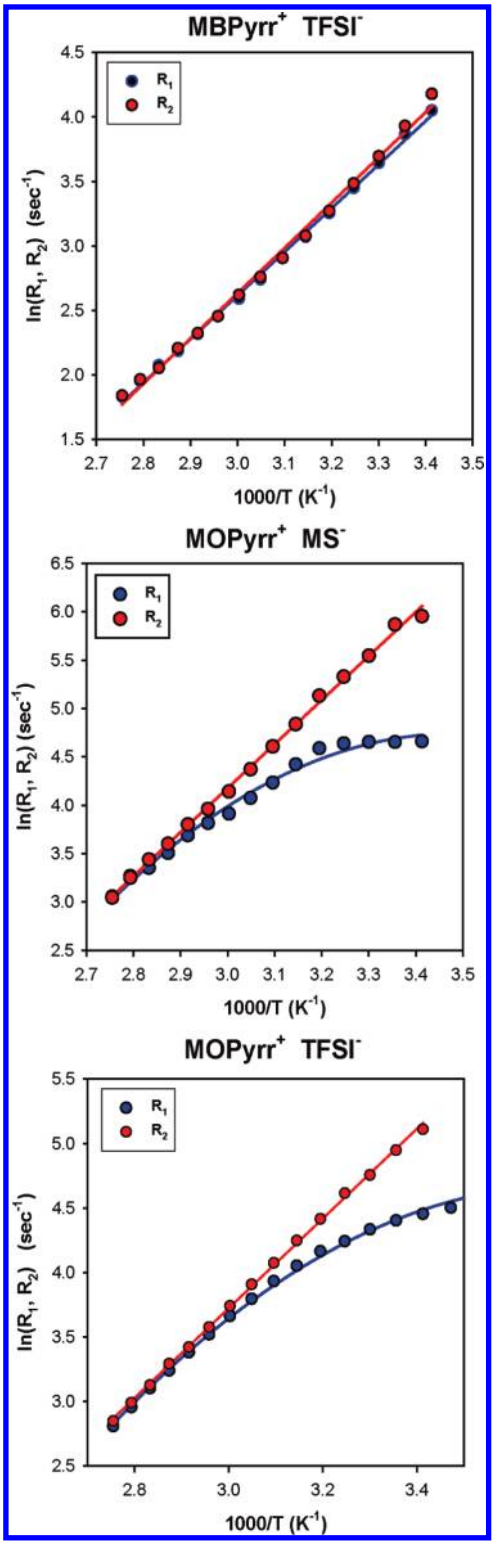

Figure 3. The ^{14}N NMR R_1 (= $1/T_1$) and R_2 (= $1/T_2$) relaxation rates as a function of temperature for different pyrrolidinium cation based IL. The linear regression to the R_2 relaxation rate allowed the reorientational activation energy (E_a) to be evaluated, while the nonlinear fit for R_1 is provided for visual aid only.

and the $TBOA^+$ cations will have small reorientational anisotropies similar to $NOENM_2E$, supporting the use of an isotropic reorientational model for these cations. On the other hand, MD simulations for the ionic liquid *N*-methyl-*N*-propylpyrrolidinium ($MPPyrr^+$) $TFSI^-$ (which is similar to the MBPyrr+ cation in this work) revealed anisotropic reorientation with the plane of the pyrrolidinium ring showing the slowest reorientational time.[51] Anisotropic molecular reorientation has also been observed in MD simulations of imidazolium cations.[52] The lengthening of the alkyl chain in the $MOPyrr^+$ cation is predicted to further increase this reorientation anisotropy for the axis along the chain vector, in comparison to $MPPyrr^+$. These MD results suggests that an anisotropic molecular reorientational model[41,42] would be more suited for the analysis of the ^{14}N NMR relaxation in pyrrolidinium cations, but as noted in the Experimental Section this incorporates additional unknown fitting parameters which are not warranted at this time. It should be noted that the R_2/R_1 method can still be used for a more complex anisotropic reorientational model, but the simple quadratic in eq 5 becomes much more complex.

The energy of activation E_a can be determined from the temperature variation of τ assuming the rotational motions can be represented by the Arrhenius function:

$$\tau = \tau_0 \exp^{-E_a/RT} \qquad (6)$$

where R is the gas constant, T is the temperature in Kelvin, and τ_0 is a preexponential factor. The measured E_a values are given in Table 1, and can be compared to those determined from the temperature dependence of the R_2 relaxation rates. The errors in the τ-derived E_a are larger due to the propagation of errors through both the R_2/R_1 ratio in eq 5, as well as the reduced number of temperatures available for the regression due to the 5% cutoff imposed (described above). There is clearly a discrepancy between E_a determined using the R_2 or τ correlations (Table 1). The underlying reason for this difference (considering they are extracted from the same relaxation data) has yet to be fully resolved. The most likely explanation is that there exists a temperature variation of the ^{14}N quadrupolar coupling constant P_Q (see discussion below) *in addition* to the temperature variation of the motional correlation time τ (eq 6). This problem is well described in the original R_2/R_1 ratio paper of Stringfellow and Farrar.[47] Attempting to extract a single E_a from the temperature variation of $\ln(R_2)$ (even though it gives a reasonable fit) assumes either a temperature independent P_Q or a temperature independent τ. By utilizing the R_2/R_1 method, no such restrictions apply as only the temperature dependence of τ would be retained in solution of eq 5.

Temperature Variation of the Quadrupolar Coupling. Recall that the evaluation of τ using the R_2/R_1 method makes no assumptions concerning the strength of the quadrupolar coupling, since P_Q is no longer present in eq 5. Therefore, the derived τ values can be reintroduced into either the R_1 or the R_2 relationships in eq 1 to extract P_Q. Figure 6 shows the variation of P_Q with increasing temperature. In general, P_Q was typically <100 kHz, reflecting the relatively high structural symmetry around the nitrogen, and is of similar magnitude to that reported for trimethylcholine.[53] All of the ILs studied herein displayed a decrease in P_Q with increasing temperature, while the ILs containing MS^- anions showed the most dramatic variations with respect to temperature. It has been suggested that the temperature-dependence of P_Q arises from the error introduced by evaluating τ near the extreme narrowing limit ($R_2 \approx R_1$). This does not appear to be the explanation, however, since the largest temperature variations in P_Q occurred at the lower temperatures, for

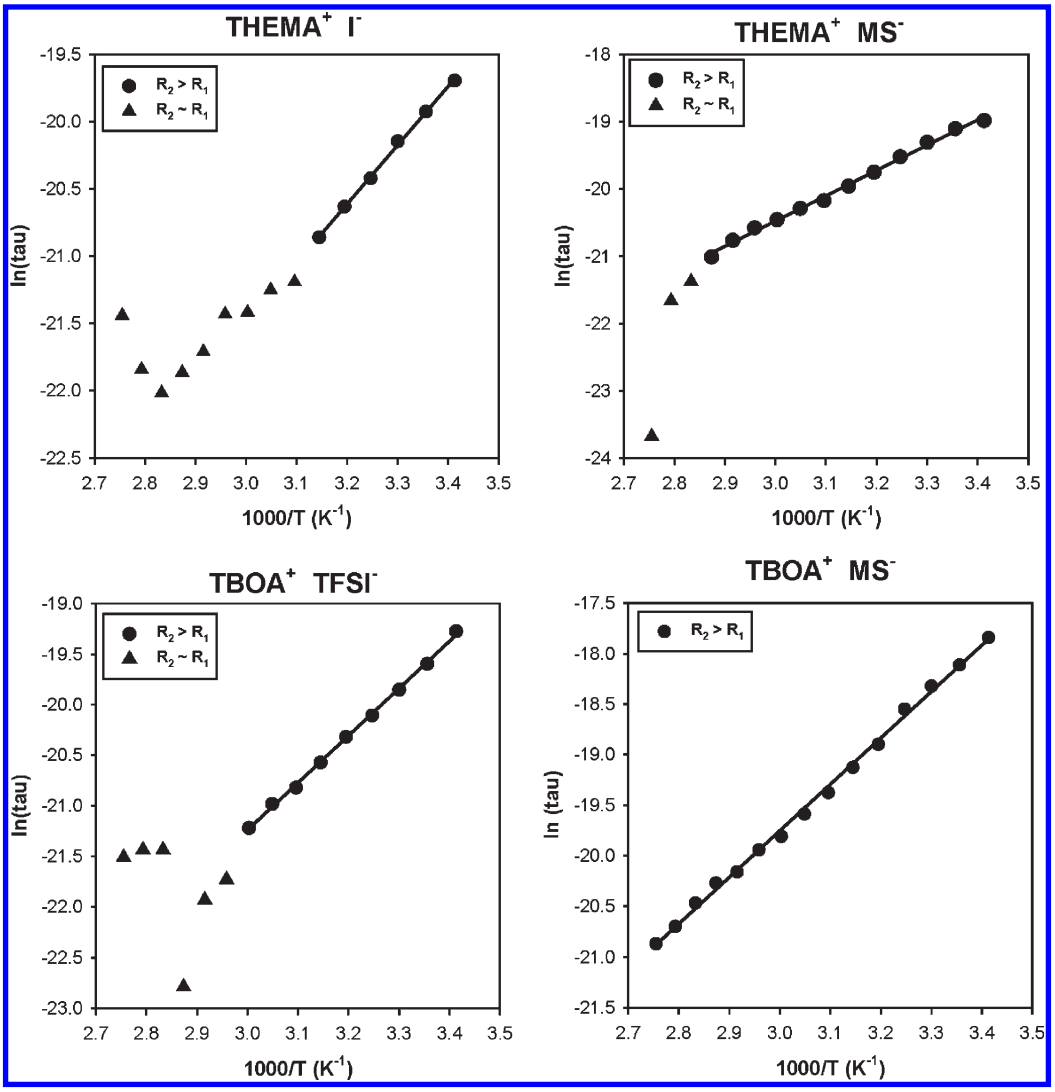

Figure 4. The temperature variation of the measured molecular reorientational correlation times for the ammonium based IL. The (●) symbols are for temperatures where R_2 is >5% larger than R_1, while (▲) are for temperatures this cutoff was not satisfied ($R_2 \approx R_1$). Additional details are provided in the text.

situations where the R_2/R_1 ratio of relaxation rates was clearly not in the extreme narrowing limit. Another possibility is that there is a mixture of different motions (spectral densities) contributing to the relaxation described in eq 1 with more than a single correlation time. While this is a possibility, the dominance of the ^{14}N quadrupolar relaxation requires that only those dynamics that produce fluctuations to the ^{14}N EFG tensor will be important.

There are numerous reports of temperature-dependent ^{14}N NMR quadrupolar coupling constants. For example, isocyanomethane,[47] *N*-methylacetamide,[54] or neat *N*-methylacetamide, and methyl isocyanide dissolved in liquid crystals[54,55] all show a temperature variation of ^{14}N P_Q that results from intermolecular interactions, hydrogen bonding, or cluster formation. Recent ab initio calculations of the ^{14}N QCC in methylpurines were able to determine the relative impact of solution structure, solvent, concentration, and complexation on the coupling parameter in that system.[56] The observation that the ^{14}N P_Q changes with the identity of the anion, clearly that intermolecular interactions are present. In addition, it is known that conformational isomerization is readily occurring in the ring structure of the pyrrolidinium ILs.[57] Whether or not such structural changes or formation of ion pairs is responsible for the changes in the ^{14}N P_Q with anion identity, or the observed temperature variation in these ILs remains to be explored and will be the focus of future research efforts in our laboratory.

Determination of Effective Molecular Volume. The NMR correlation times can be related to macroscopic properties using the Debye−Stokes−Einstein (DSE) hydrodynamic theory model involving the local microviscosity (η) through the following:[19,20,58]

$$\tau = \frac{\eta V_{\text{eff}}}{kT} + \tau_0 \qquad (7)$$

The effective volume ($V_{\text{eff}} = fV$) is related to the true molecular volume using the coupling factor f, which is a function of the molecular shape as well as the hydrodynamic boundary conditions. The factor τ_0 is argued to be related to either the free rotor correlation times or related to cross-correlation function between kinetic and torque-like terms.[59,60] In some examples, τ_0 has been assumed to be small and was ignored, such that effective volumes

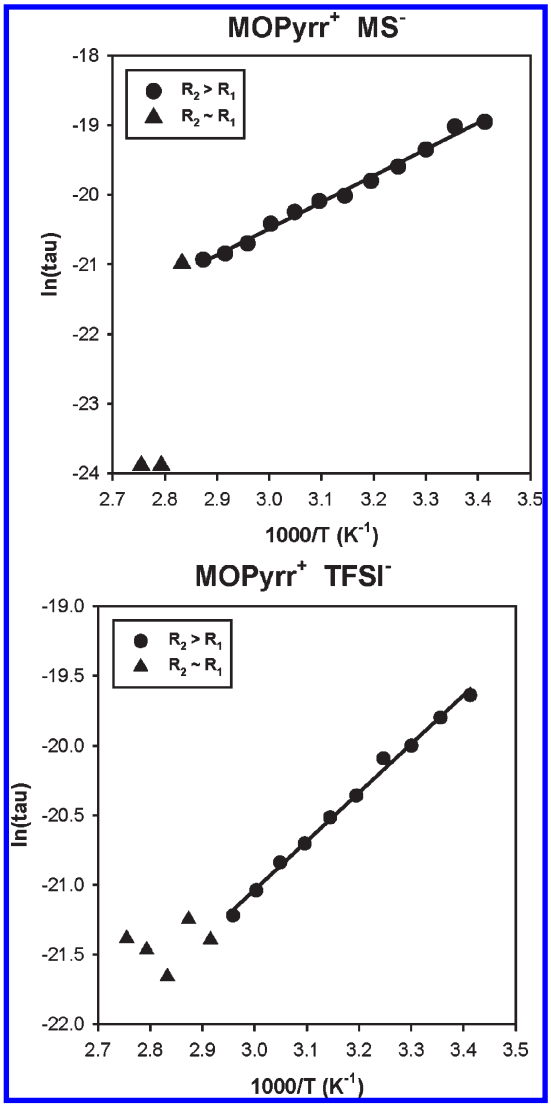

Figure 5. The temperature variation of the measured molecular reorientational correlation times for the pyrrolidinium based IL. The (●) symbols are for temperatures, where R_2 is >5% larger than R_1, while (▲) are for temperatures this cutoff was not satisfied ($R_2 \approx R_1$). Additional details are provided in the text.

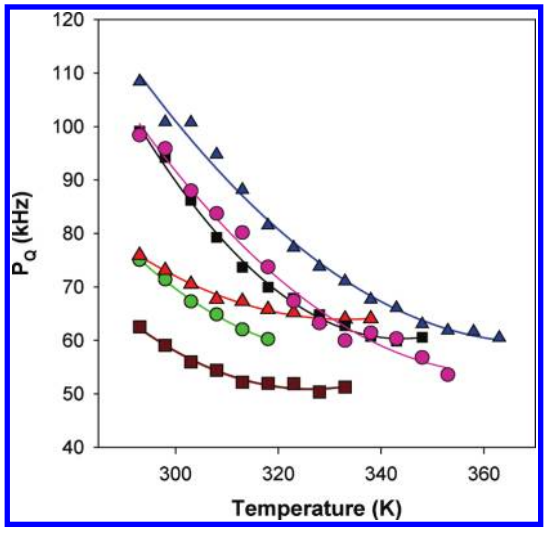

Figure 6. The temperature variation of the quadrupolar coupling product for the acyclic ammonium and cyclic pyrrolidinium ionic liquids, $THEMA^+ I^-$ (green ●), $THEMA^+ MS^-$ (■), $TBOA^+ MS^-$ (blue ▲), $TBOA^+ TFSI^-$ (Maroon ■), $MOPyrr^+ MS^-$ (pink ●) and $MOPyrr^+ TFSI^-$ (red ▲). The nonlinear fit is provided for visual aid only.

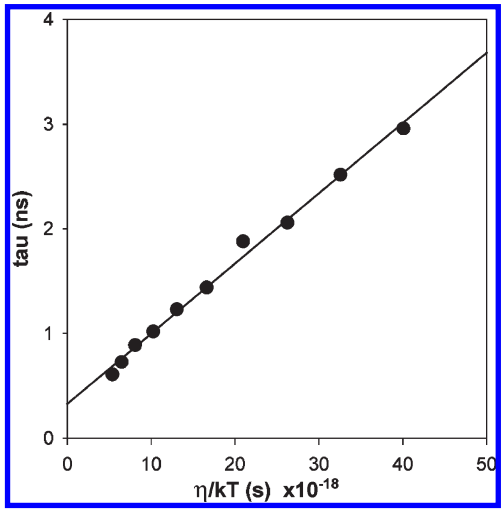

Figure 7. The variation of the ^{14}N NMR determined molecular reorientation correlation times as a function of viscosity and inverse temperature for $MOPyrr^+ TFSI^-$.

are estimated from a single viscosity value. Ignoring τ_0 does not appear to be appropriate for ILs, and was not used here. Instead, V_{eff} was evaluated from a plot of τ versus η/kT, where we have assumed that the V_{eff} and f are temperature independent. Unfortunately, this type of analysis requires the viscosity temperature variation to be known, which is not the case for the majority of the series of IL reported here. However, the temperature dependence for $[MOPyrr]^+TFSI^-$ and $[MBPyrr]^+TFSI^-$ has been determined by Salminen and co-workers.[61,62] Figure 7 shows the η/kT correlation ($r^2 = 0.9940$) for $[MOPyrr]^+TFSI^-$, supporting the assumed relationship of eq 7. A V_{eff} of 0.067 nm^3 was determined from the slope, while the intercept gave the preexponential term τ_0 of +0.33 ns. This measured V_{eff} is significantly smaller than the 0.580 nm^3 volume predicted from gas phase calculations, to give a coupling factor of $f = 0.1155$. This coupling factor is actually larger than those previous estimated for imidazolium ILs using both dielectric and NMR spectroscopy.[19,63] Improvements in the DSE description can be pursued by incorporating the nonspherical shape of the $[MOPyrr]^+TFSI^-$ (which has an ovality of 1.38) such as described by Hu and Zwanzig[64] and Youngren.[65] These modifications still resulted in a relatively small V_{eff}, placing the coupling factor in the boundary slip conditions. In the previous section on the ^{14}N P_Q temperature variation we argued that thermally activated molecular rearrangements may be responsible for the observed temperature variations. This argument suggests that the temperature invariant V_{eff} assumption may not be correct, and that further development of eq 7 needs to be pursued. We are currently investigating the correlation of the molecular correlation times τ with the with the ILs molecular volume using a Volume Based Approach (VBA),[66,67] as previously demonstrated for density, viscosity, and diffusion coefficients. These correlation results will be presented elsewhere.

CONCLUSIONS

This work demonstrates that ^{14}N NMR spectroscopy may be used to probe the molecular dynamics in acyclic ammonium and cyclic pyrrolidinium ionic liquids. By determining both the spin−lattice and spin−spin relaxation rates using the R_2/R_1 method, the correlation times for the reorientation of the cation were directly evaluated. This method does not require the determination of another correlation time within the molecule. The measured cation reorientational correlation times were a function of both the cation size and the anion identity. The temperature variation of the reorientational correlation times allowed activation energies for this dynamic process to be determined. Similar ^{14}N NMR experiments should be possible for other nitrogenous ionic liquids that contain moderate nitrogen quadrupolar coupling constants. For example, diethylpyridinium had a QCC = +2.5 MHz, but stilled revealed an observable ^{14}N resonance.[33] By combining the molecular reorientational correlation times with viscosity data the effective molecular volume for the pyrrolidinium cation was estimated, and revealed slip boundary conditions. The ^{14}N NMR results for this IL series provide a basis for comparison involving future studies involving more complex mixtures or investigations into IL/surface interactions.

ASSOCIATED CONTENT

Supporting Information. Include the synthetic details of the precursor ILs and the ILs previously described in literature. This material is available free of charge via the Internet at http://pubs.acs.org.

AUTHOR INFORMATION

Corresponding Author
*E-mail: tmalam@sandia.gov.

ACKNOWLEDGMENT

This research was funded by the U.S. DOE, Office of Basic Energy Sciences, under Award ID DE-SC001951 and ER46657. Sandia National Laboratories is a multiprogram laboratory operated by Sandia Corporation, a wholly owned subsidiary of Lockheed Martin Company, for the U.S. Department of Energy's National Nuclear Security Administration under Contract No. DE-AC04-94AL85000.

REFERENCES

(1) Murali, S.; Dreyer, D. R.; Valle-Vigon, P.; Stoller, M. D.; Zhu, Y.; Morales, C.; Fuertes, A. B.; Bielawski, C. W.; Ruoff, R. S. *Phys. Chem. Chem. Phys.* **2011**, *13*, 2652.
(2) Wishart, J. F. *Energy Environ. Sci.* **2009**, *2*, 956.
(3) Kim, T. Y.; Lee, H. W.; Stoller, M. D.; Dreyer, D. R.; Bielawski, C. W.; Ruoff, R. S.; Suh, K. S. *ACS Nano* **2011**, *5*, 436.
(4) Karadas, F.; Atilhan, M.; Aparicio, S. *Energy Fuels* **2010**, *24*, 5817.
(5) Zhao, H. *Chem. Eng. Commun.* **2006**, *193*, 1660.
(6) Uzagare, M. C.; Salunkhe, M. *Asian Chem. Lett.* **2004**, *8*, 269.
(7) Bermúdez, M.-D.; Jiménez, A.-E.; Sanes, J.; Carrión, F.-J. *Molecules* **2009**, *14*, 2888.
(8) Tan, S. S. Y.; MacFarlane, D. R. *Top. Curr. Chem.* **2009**, *290*, 311.
(9) Li, Z.; Jia, Z.; Luan, Y.; Mu, T. *Curr. Opin. Solid State Mater. Sci.* **2008**, *12*, 1.
(10) Zhou, Y. *Curr. Nanosci.* **2005**, *1*, 35.
(11) Giernoth, R. *Top. Curr. Chem.* **2007**, *276*, 1.
(12) Mele, A.; Romanó, G.; Giannone, M.; Ragg, E.; Fronza, G.; Raos, G.; Marcon, V. *Angew. Chem., Int. Ed.* **2006**, *45*, 1123.
(13) Chiappe, C. *Monatsh. Chem.* **2007**, *138*, 1035.
(14) Hardacre, C.; Holbrey, J. D.; Nieuwenhuyzen, M.; Youngs, T. G. A. *Acc. Chem. Res.* **2007**, *40*, 1146.
(15) Roth, C.; Peppel, T.; Fumino, K.; Köckerling, M.; Ludwig, R. *Angew. Chem.* **2010**, *49*, 10221.
(16) Hamaguchi, H.-O.; Ozawa, R. *Adv. Chem. Phys.* **2005**, *131*, 85.
(17) Giernoth, R. *Top. Curr. Chem.* **2009**, *290*, 263.
(18) Burrell, G. L.; Burgar, I. M.; Separovic, F.; Dunlop, N. F. *Phys. Chem. Chem. Phys.* **2010**, *12*, 1571.
(19) Wulf, A.; Ludwig, R.; Sasisanker, P.; Weingärtner, H. *Chem. Phys. Lett.* **2007**, *439*, 323.
(20) Huang, J.-F.; Chen, P.-Y.; Sun, I.-W.; Wang, S. P. *Inorg. Chim. Acta* **2001**, *320*, 7.
(21) Judeinstein, P.; Iojoiu, C.; Sanchez, J.-Y.; Ancian, B. *J. Phys. Chem. B* **2008**, *112*, 3680.
(22) Imanari, M.; Uchida, K.-i.; Miyano, K.; Seki, H.; Nishikawa, K. *Phys. Chem. Chem. Phys.* **2010**, *12*, 2959.
(23) Tokuda, H.; Tsuzuki, S.; Susan, M. A. B. H.; Hayamizu, K.; Watanabe, M. *J. Phys. Chem. B.* **2006**, *110*, 19593.
(24) Álvarez, V. H.; Dosil, N.; Gonzalez-Cabaleiro, R.; Mattedi, S.; Martin-Pastor, M.; Iglesias, M.; Navaza, J. M. *J. Chem. Eng. Data* **2010**, *55*, 625.
(25) Tokuda, H.; Hayamizu, K.; Ishii, K.; Susan, M. A. B. H.; Watanbe, M. *J. Phys. Chem. B* **2004**, *108*, 16593.
(26) Tokuda, H.; Hayamizu, K.; Ishii, K.; Susan, M. A. B. H.; Watanbe, M. *J. Phys. Chem. B* **2005**, *2005*, 6103.
(27) Tokuda, H.; Ishii, K.; Susan, M. A. B. H.; Tsuzuki, S.; Hayamizu, K.; Watanbe, M. *J. Phys. Chem. B* **2006**, *110*, 2833.
(28) Menjoge, A.; Dixon, J.; Brennecke, J. F.; Maginn, E. J.; Vasenkov, S. *J. Phys. Chem. B* **2009**, *113*, 6353.
(29) Iacob, C.; Sangoro, J. R.; Papdopoulos, P.; Schubert, T.; Naumov, S.; Valiullin, R.; Käregr, J.; Kremer, F. *Phys. Chem. Chem. Phys.* **2010**, *12*, 13798.
(30) Waechtler, M.; Sellin, M.; Stark, A.; Akcakayiran, D.; Findenegg, G.; Gruenberg, A.; Breitzke, H.; Buntkowsky, G. *Phys. Chem. Chem. Phys.* **2010**, *12*, 11371.
(31) Le Bideau, J.; Gaveau, P.; Bellayer, S.; Nèouze, M.-A.; Vioux, A. *Phys. Chem. Chem. Phys.* **2007**, *9*, 5419.
(32) Forsyth, M.; Kemp, T. F.; Howlett, P. C.; Sun, J.; Smith, M. E. *J. Phys. Chem. C* **2008**, *112*, 13801.
(33) Ghesquière, D.; Chachaty, C. *Org. Magn. Reson.* **1977**, *9*, 392.
(34) Brenna, S.; Posset, T.; Furrer, J.; Blümel, J. *Chem.—Eur. J.* **2006**, *12*, 2880.
(35) Sakaebe, H.; Matsumoto, H. *Electrochem. Commun.* **2003**, *5*, 594.
(36) Howlett, P. C.; MacFarlane, D. R.; Hollenkamp, A. F. *Electrochem. Solid-State Lett.* **2004**, *7*, A97.
(37) Berger, S.; Braun, S. *200 and More NMR Experiments*; Wiley-VCH: Weinheim, 2004.
(38) Sun, J.; MacFarlane, D. R.; Forsyth, M. *Ionics* **1997**, *3*, 365.
(39) Sun, J.; Forsyth, M.; MacFarlane, D. R. *J. Phys. Chem. B* **1998**, *102*, 8858.
(40) Abragam, A. *Principles of Nuclear Magnetism*; Oxford University Press: Oxford, 1961.
(41) Canet, D. *Concepts Magn. Reson.* **1998**, *10*, 219.
(42) Witanowski, M.; Stefaniak, L.; Januszewski, H.; Saluvere, T.; Webb, G. A. *Adv. Mol. Relax. Proc.* **1973**, *5*, 169.
(43) Stringfellow, T. C.; Farrar, T. C. *J. Phys. Chem.* **1995**, *99*, 3889.
(44) Carper, W. R. *Concepts Magn. Reson.* **1998**, *11*, 51.
(45) Keller, C. E.; Piersma, B. J.; Mains, G. J.; Carper, W. R. *Inorg. Chem.* **1994**, *33*, 5601.
(46) This relationship is equivalent to eq 4 in ref 44.
(47) Stringfellow, T. C.; Farrar, T. C. *J. Chem. Phys.* **1995**, *102*, 9465.
(48) Burrell, G. L.; Burgar, I. M.; Gong, Q.; Dunlop, N. F.; Separovic, F. *J. Phys. Chem. B* **2010**, *114*, 11436.

(49) Chung, S. H.; Lopato, R.; Greenbaum, S. G.; Shirota, H.; Castner, E. W., Jr.; Wishart, J. F. *J. Phys. Chem. B.* **2007**, *111*, 4885.
(50) Siqueira, L. J. A.; Ribeiro, M. *J. Phys. Chem. B.* **2007**, *111*, 11776.
(51) Borodin, O.; Smith, G. D. *J. Phys. Chem. B* **2006**, *110*, 11481.
(52) Urahata, S. M.; Ribeiro, M. C. C. *J. Chem. Phys.* **2005**, *122*, 024511.
(53) Koga, K.; Kanazawa, Y. *J. Phys. Chem.* **1983**, *87*, 5219.
(54) Ludwig, R.; Weinhold, F.; Farrar, T. C. *J. Phys. Chem. A* **1997**, *101*, 8861.
(55) Barbara, T. *Mol. Phys.* **1985**, *54*, 651.
(56) Kotsyubynskyy, D.; Gryff-Keller, A. *J. Phys. Chem. A* **2007**, *111*, 1179.
(57) Umebayahi, Y.; Mitsugi, T.; Fujii, K.; Seki, S.; Chiba, K.; Yamamoto, H.; Lopes, j. N. C.; Padua, A. A. H.; Takeuchi, M.; Kanzaki, R.; Ishiguro, S.-i. *J. Phys. Chem. B.* **2009**, *113*, 4338.
(58) Larive, C. K.; Lin, M.; Kinnear, B. S.; Piersma, B. J.; Keller, C. E.; Carper, W. R. *J. Phys. Chem. B* **1998**, *102*, 1717.
(59) Evilla, R. F.; Robert, J. M.; Whittenburg, S. L. *J. Phys. Chem.* **1989**, *93*, 6550.
(60) Rudakoff, G.; Oehme, K.-L. *Chem. Phys. Lett.* **1978**, *54*, 342.
(61) Saliminen, J.; Papaiconomou, N.; Kumar, R. A.; Lee, J.-M.; Kerr, J.; Newman, J.; Prausnitz, J. M. *Fluid Phase Equilib.* **2007**, *261*, 421.
(62) 2, N. (2011).
(63) Huang, M.-M.; Bulut, S.; Krossing, I.; Weingärtner, H. *J. Chem. Phys.* **2010**, *133*, 101101.
(64) Hu, C.-M.; Zwanzig, R. *J. Chem. Phys.* **1974**, *60*, 4354.
(65) Youngren, G. K.; Acrivos, A. *J. Chem. Phys.* **1975**, *63*, 3846.
(66) Bogdanov, M. G.; Kantlehner, W. *Z. Naturforsch.* **2009**, *64b*, 215.
(67) Slattery, J. M.; Daguenet, C.; Dyson, P. J.; Schubert, T. J. S.; Krossing, I. *Angew. Chem.* **2007**, *119*, 5480.